ERJ open research
THE BEST IN OPEN ACCESS BASIC, TRANSLATIONAL & CLINICAL RESPIRATORY RESEARCH

Early View

Original research article

Vascular remodelling in IPF patients and its detrimental effect on lung physiology: potential role of endothelial to mesenchymal transition (EndMT)

Archana Vijay Gaikwad, Wenying Lu, Surajit Dey, Prem Bhattarai, Collin Chia, Josie Larby, Greg Haug, Stephen Myers, Jade Jaffar, Glen Westall, Gurpreet Kaur Singhera, Tillie-Louise Hackett, James Markos, Mathew Suji Eapen, Sukhwinder Singh Sohal

Please cite this article as: Gaikwad AV, Lu W, Dey S, *et al*. Vascular remodelling in IPF patients and its detrimental effect on lung physiology: potential role of endothelial to mesenchymal transition (EndMT). *ERJ Open Res* 2022; in press (https://doi.org/10.1183/23120541.00571-2021).

Vascular remodelling in IPF patients and its detrimental effect on lung physiology: potential role of endothelial to mesenchymal transition (EndMT)

Archana Vijay Gaikwad[1,2], Wenying Lu[1,2], Surajit Dey[1], Prem Bhattarai[1], Collin Chia[1,3,] Josie Larby[1,3], Greg Haug[1,3], Stephen Myers[1], Jade Jaffar[4,5], Glen Westall[4,5], Gurpreet Kaur Singhera[6,7], Tillie-Louise Hackett[6,7], James Markos[1,2], Mathew Suji Eapen[1,2#], Sukhwinder Singh Sohal[1#]

[1]Respiratory Translational Research Group, Department of Laboratory Medicine, School of Health Sciences, College of Health and Medicine, University of Tasmania, Launceston, Tasmania, Australia, 7248

[2]National Health and Medical Research Council (NHMRC) Centre of Research Excellence (CRE) in Pulmonary Fibrosis, Australia.

[3]Department of Respiratory Medicine, Launceston General Hospital, Launceston, Tasmania 7250, Australia.

[4]Department of Allergy, Immunology and Respiratory Medicine, The Alfred Hospital, Melbourne, Australia.

[5]Department of Immunology and Pathology, Monash University, Melbourne, Australia

[6]Department of Anaesthesiology, Pharmacology and Therapeutics, University of British Columbia, Vancouver, BC, Canada.

[7]Centre for Heart Lung Innovation, St. Paul's Hospital, Vancouver, BC, Canada.

#Equal contributors

***Corresponding Author**

Dr Sukhwinder Singh Sohal

Respiratory Translational Research Group

Department of Laboratory Medicine, School of Health Sciences,

College of Health and Medicine, University of Tasmania

Locked Bag – 1322, Newnham Drive

Launceston, Tasmania 7248, Australia

Telephone number: +61 3 6324 5434

Email: sssohal@utas.edu.au

Abstract

Background

IPF is a progressive, irreversible fibrotic interstitial lung disease. We performed size-based quantitation of pulmonary arterial remodelling in IPF, examined the role of EndMT and effects on lung physiology.

Methods

Resected lung tissues from 11 normal controls (NC), and 13 IPF patients, were differentially stained using the Movat Pentachrome technique. Size-based classification for pulmonary arteries was conducted in NC and IPF tissues. For each pulmonary artery, arterial size, luminal diameter, thickness of the intima, media, adventitia, and elastin deposition was quantified using Image ProPlus7.0 software. In addition, immunohistochemical staining was performed for EndMT markers and collagen.

Results

Large and medium size arterial numbers were significantly reduced in IPF compared to NC ($p<0.0001$). Intima thickness was highest in the arterial range of 200-399μm and 600-1000μm ($p< 0.0001$), while medial and adventitial thickness was significant across 200-1000μm ($p<0.05$) compared to NC. Medial thickness was found to significantly affect the diffusing capacity of the lungs for carbon monoxide (DLCO) ($r'=-0.8$, $p=0.01$). Total arterial elastin in IPF was higher across all arterial ranges except 100-199μm in IPF than NC, with the greatest differences in 200-399μm ($p<0.001$) and 600-1000μm ($p<0.001$). Total elastin also negatively correlated with DLCO ($r'=-0.63$, $p=0.04$) in IPF. An increase in EndMT markers and collagen type I/ IV was observed.

Conclusions

This is the first study demonstrating size-based differences in pulmonary arteries in IPF and its detrimental effect on lung physiology. The process of EndMT might be central to these vascular remodelling changes and could be a potential novel therapeutic target.

Key Words

Idiopathic pulmonary fibrosis, EndMT, Pulmonary hypertension, Pulmonary artery, and Vascular remodelling

Introduction

Idiopathic pulmonary fibrosis (IPF) is a progressive chronic interstitial lung disease (ILD) associated with irreversible lung fibrosis. IPF is a deadly disease, with mortality rates averaging 3.8 years from diagnosis [1, 2]. Currently, IPF affects more than 3 million people worldwide, which forms a substantial burden on healthcare [3]. Honeycombing and usual interstitial pneumonia (UIP) are some of the common observations of IPF lung when detected through high-resolution computed tomography [4]. Despite unknown aetiology, environmental, microbial factors, and genetic susceptibility are associated with IPF pathogenesis[1, 4]. IPF pathology results from repeated injury to the lung interstitium, causing aberrant repair, leading to intense interstitial fibrosis and restricted gas exchange [5]. Several cells, including alveolar type II pneumocytes, endothelial cells, pericytes, fibrocytes, macrophages and mast cells, are crucial contributors to IPF pathogenesis. These cells promote the accumulation and proliferation of fibroblasts through several but undeciphered mechanisms and uneven deposition of extracellular matrix (ECM), culminating in irreversible lung parenchyma scarring and damage [6].

IPF patients are prone to abnormal structural changes in the pulmonary arteries, leading to pulmonary hypertension (PH) [7]. Past findings suggest lower blood vessel formation in fibrotic versus non-fibrotic areas, displaying considerable vascular heterogeneity across the IPF lung [8, 9]. Abnormal structural modifications of the vasculature such as complete occlusion or narrowing of the vessels by scarred tissues, plexiform lesions, proliferative intima, and thickening of smooth muscle layers are some of the mainstays IPF pathology [8, 10]. Interestingly, the low diffusing capacity of the lungs for carbon monoxide (DLCO) observed in IPF patients are also linked to PH development, comorbidity observed in 30-80% of IPF patients [11]. Colombat et al. [12] suggested that occlusive venopathy in the non-fibrotic area of IPF lungs caused a reduction in pulmonary capillary blood volume, which was linked to lower DLCO in IPF-PH patients [13]. Furthermore, vascular remodelling was also observed to affect forced vital capacity (FVC) in IPF patients [14], though some studies have reported otherwise [11, 15].

Currently, there is little evidence on systematic morphometric analysis of arterial vascular remodelling in patients with IPF. For example, Parra et al [14] morphometrically evaluated the internal luminal area and the perimeter of medium and large arteries in lung tissue from IPF patients. They suggested significant links between histological UIP patterns and vascular remodelling changes. Decreasing internal luminal area and increasing wall thickness of both

medium and large arteries was mainly noted; but, the study was semiquantitative[14]. A more recent study by Kinoshita et al. used broad classified arterial ranges to identify increases in individual layer thickness in IPF and idiopathic pleuroparenchymal fibroelastosis patients compared to control lungs tissues. The study, however, lacked association with physiological outcomes [16].

In the current study, we employed a comprehensive size-based classification approach to study normal and IPF arteries, and we provided data on absolute counts against a cohort of normal healthy controls. In addition, we analysed the thickness of each layer within arteries and have studied their effects on physiological function such as FVC, DLCO and smoking history in IPF patients. Our data implicates that increased deposition of elastin, collagen-type I and IV could contribute to the arterial thickness in IPF lung. Finally, we illustrate the possible role of EndMT activity in vascular remodelling.

Material and methods

Study population

Explant human lung tissues from thirteen patients diagnosed with IPF were obtained during lung transplantation (Alfred Health Biobank Melbourne, ethics ID: 336-13), and none were on anti-fibrotic treatment. All patients had pathologist-verified histopathology reports of usual interstitial pneumonia (UIP). In addition, tissues from eleven healthy normal control (NC) subjects consisting of small airways and parenchymal areas were provided by James Hogg Lung Registry, the University of British Columbia (ethics ID: H00-50110). This cohort consisted of patients who had died of causes other than pulmonary diseases. Detailed subject demographic information is provided in Table 1. All the functional data was collected before the lung transplantation.

Movat's Pentachrome staining

Formalin-fixed, paraffin-embedded tissue sections were cut (3.5-micron). First, dewaxing of the tissue sections was done in Xylene twice for 3 minutes, followed by gradually hydration using 100%, 95%, 70% ethanol, and running tap water. Next, tissue sections were stained with Movat Pentachrome staining kit (Modified Russell-Movat-ab245884, Abcam, Australia) as per manufacturer instructions. The staining differentiates arterial structural morphology based on colours such as collagen (yellow to red), elastin (black-blue) and nuclei (blue), muscle (red), mucin (bright blue), and fibrin (bright red) (figure 1 and 2).

Immunohistochemical staining for mesenchymal markers

Lung tissue sections were deparaffinized in xylene and antigen retrieval using target retrieval citrate buffer pH 6.0 (Dako S2369) for 15 min. Tissues were immunostained with polyclonal rabbit anti-human S100A4 (1:1000; Dako A5114) mouse monoclonal VE-cadherin (CD144) (1:150; Thermofisher 14144982), vimentin, monoclonal mouse (1:200; Dako, M7020), mouse monoclonal anti-N cadherin (1:100; Abcam ab98952) monoclonal mouse anti-α-SMA (1:500, M0851, Dako), collagen-type I (1:200, Abcam ab34710), rabbit polyclonal and collagen-type IV (1:200, Abcam ab6586), rabbit polyclonal for 60 mins followed by secondary HRP rabbit/ mouse antibodies (Dako K5007) treatment for a further 30 mins. The protein markers were visualized as brown after adding DAB substrate and counterstained for the nucleus with Hematoxylin.

Pulmonary arterial, classification, and counts

All images were captured using a Leica DM 500 microscope and Leica IC50W digital camera. Pulmonary arteries were first distinguished for morphometric analysis based on their rounded structure and thickness, with veins thinner and elongated (figure 1a). The pulmonary arteries also had at least two defined elastin layers than veins with only a single.

For arterial classification, measurements for at least five arteries for each size was carried out. Each arterial image from NC and IPF was taken with a 4x objective following a vertical uni-direction, avoiding overlap. External length (one end to the other end of adventitia) and luminal length (one end to another end of intima layer margin) were measured (figure 1b) using measurement tools in the image ProPlus 7.0 software. Based on the size measurements, arteries were segregated into six groups, 100-1000μm, interspaced at 100μm, and total arterial length to luminal length ratios was done to determine the degree of vascular remodelling in IPF (figure1b). In addition, the arterial numbers per mean percent of tissue density were counted for all classified arterial sizes in IPF and NC.

Pulmonary total arterial and layer thickness measurement

The length of all three layers of arteries represented the total arterial thickness. To better assess arterial thickness across arterial sizes, separate magnifications were used; for instance, 63x objective for smaller 100-199μm arteries, 40x for 200-399μm, 20x for 400-599 μm and 10x for 600-1000μm respectively. Similar magnifications were used to quantify thickness of individual layers. Subsequently, non-overlapping images were taken for all arterial sizes, and five images

per arterial size per subject was randomly selected using an online random number generator. All the analysis was done with observer (AVG) blinded to subject and diagnosis.

Strategies for arterial thickness measurement were done as previously described [17]. In brief, the area of interest from each layer was manually drawn using imaging software tools. For intima measurements, thickness measurements from the outer luminal to the inner elastin layer were considered. Media layer thickness included the external layer of the inner elastin membrane and internal lining of the external elastin membrane, while areas from the media's external elastin layer to the arteries outermost connective tissue were considered adventitial thickness measurements. Based on arterial orientation, a horizontal, vertical, or curved tool was selected using the software measurement tools and, the average distance between the selected layer margins was calculated using an automated distance calculator programme within the image ProPlus 7.0 software.

Pulmonary arterial elastin measurement

Image acquisition and randomisation were followed similarly to thickness measurements. For total arterial measurements, the start of the outer end of the intima facing the lumen to the outer border of adventitia was manually selected using imaging software. For quantification of elastin, the total dark object was counted from the area of interest, and then elastin colour (black to blue/black) from the area of interest was counted. A similar strategy was used to measure intima, media, and adventitia layer elastin. Percentage elastin was calculated using the following formula.

$$\text{Pulmonary arterial each layer percentage elastin} = \left(\frac{\text{number of selected colour objects from the area of interest}}{\text{total number of the dark object from the area of interest}}\right) \quad X100$$

Statistical analysis

All cross-sectional data were tested for their normal distributions using the D'Agostino-Pearson omnibus normality test. Analyses of variance were performed using ordinary one-way ANOVA using Bonferroni multiple comparison tests, which compared mean and standard deviation across all the interest groups; specific group differences with correction for multiple comparisons were assessed using Dunn's test. Finally, for multi-variable correlations, we

performed regression analyses using Spearman's rank test. All analysis was done using GraphPad prismV9, with a p-value ≤ 0.05 being considered significant.

Results

Morphological assessment of pulmonary arteries

Large and medium-size arterial numbers were significantly reduced in IPF compared to NC. Compared to arteries in control lungs, patients with IPF showed structural changes such as endothelial proliferation into the lumen, muscular hypertrophy of the intima and medial layer, proliferative intima, and plexiform lesions. Also, excessive collagen and elastin deposition at adventitia was observed. Some of the arteries were completely remodelled and indistinguishably merged into surrounding tissues. Our data implicate that increased elastin and collagen deposition could contribute to the arterial thickness in IPF lung (figure 2).

Arterial structural changes and their number

A significant decrease in arterial numbers was observed across medium and larger classified arterial ranges, i.e., 200-1000μm range. Smaller artery numbers also trended lower in IPF but were non-significant compared to NC (figure 3a). The differences in total arterial length to lumen ratios in medium to larger 300-399μm and 600-1000μm size ($p<0.0001$) was more significant than 100-199μm and 200-299μm ($p<0.001$) arterial ranges compared to NC (figure 3b).

We analysed relationships between arterial number, total arterial length to lumen ratios and DLCO. We noted that total arterial number positively correlated with DLCO % predicted ($r'=0.56$, $p<0.05$) (figure 4a) while the increase in arterial length to luminal ratios negatively correlated with DLCO% predicted ($r'=-0.61$, $p=0.03$) (figure 4b). Further, we also observed no significant differences between total arterial length to lumen ratios for arteries from fibrosed and non-fibrosed areas in IPF tissues (figure 4c).

Total arterial and layer thickness in IPF patients

Thickness was measured across all the three arterial zones intima, media and adventitia in NC and IPF (figure 5a, b). Compared to NC, a two-fold increase in total thickness was found across arterial sizes, except the 100-199μm range, wherein trends were higher, though insignificantly (figure 5c). Among individual arterial layers, intima showed a more significant fold difference in IPF than NC compared to media and adventitia. Intima was thicker across all measured

arterial ranges in IPF patients, with greater significance observed in the arterial range of 200-399μm and 600-1000μm ($p<0.0001$), respectively, compared to NC (figure 5d, e, f and g). Within lower arterial ranges, both medial and adventitial thickness was distinguishably smaller in NC and IPF; however, the larger arterial range had significant increases in media with the greatest difference being in 600-1000μm ($p<0.001$) and adventitia in 400-599μm ($p<0.001$) in IPF arteries than NC.

Elastin deposition in arterial layers

The Movat Pentachrome stained elastin dark blue (figure 6a, b). In NC, elastin structures were well defined with inner and outer boundaries surrounding the media smooth muscle layer (figure 6a); however, elastin in IPF was disintegrated and scattered across and within the various layers (figure 6b). Quantitative analysis of the total arterial percent elastin was significant across arterial ranges in IPF compared to NC except for 100-199μm. The median value of percent elastin in IPF subjects averaged 20% in small and mid-sized arteries, while larger arteries had close to 40% (figure 6c). In comparison, NC had significantly lower total elastin ranging from 5-10% across arterial sizes (figure 6c). Similar trends were observed in individual arterial layer analysis of elastin, with consistent increases seen across mid [200-399 ($p<0.001$), 400-599μm ($p<0.01$)], and larger arteries [600-1000μm($p<0.001$)], however, smaller arteries showed lower significance likely due to considerable variability observed in both IPF and NC (figure 6d, e, f, g).

Arterial remodelling impact on lung physiology.

We analysed relationships between arterial thickness, elastin deposition, and lung physiological parameters through a multi-variable correlation matrix. We identified that both total thickness and total percent elastin showed a significant negative correlation to DLCO% predicted ($r'=-0.75$, $p=0.01$) and ($r'=-0.46$, $p=0.09$) respectively (figure 7a, c). Individual layer thickness negatively correlated with DLCO; intima thickness vs. DLCO % predicted ($r'=-0.57$, $p=0.05$); media thickness vs. DLCO % predicted ($r'=-0.84$, $p=<0.001$) and adventitia thickness vs DLCO %predicted ($r'=-0.75$, $p=<0.01$). The total and individual layer thickness negatively correlated to FVC (L) insignificantly (figure 7b). Similar to total elastin, individual layers elastin also showed negative correlations DLCO % predicted ($r'=-0.31$, $p=0.17$) for intima, DLCO % predicted ($r'=-0.21$, $p= 0.27$) for media and DLCO (%) predicted ($r'=-0.26$, $p=0.22$) for adventitia (figure 7d). Smoking (pack-years) affected both total and individual layer thicknesses and elastin deposition in IPF patients.

The correlation matrix between arterial elastin and thickness showed increased elastin percentage in each arterial layer correlated to their corresponding layer thickness (figure 7e).

Descriptive analysis of IPF arteries showed increase in EndMT marker expression

We observed increased expression of mesenchymal biomarkers N-Cadherin, S100A4 and vimentin in the arterial layers (intima, media, and adventitia) of IPF patients compared to NC, indicating the possible active transition of resident cells into mesenchymal traits (figures 8c, d, e, f, g, h). Furthermore, in NC, the endothelial VE-cadherin expression was explicitly observed at cell junctions, while in IPF, they were more cytoplasmic (figure 8a, b). We also observed in the arterial layers of IPF patients, an increase in myofibroblast marker α-SMA and ECM proteins collagen type-I and IV, especially pronounced in intimal areas compared to NC (figures 8i, j, k, l, m, n). In addition, the staining intensity of collagen type-I was more enhanced and widespread across the tissue than collagen type-IV, which was artery specific. Also, unlike IPF, the NC subject's collagen type IV was intact within arterial basement membrane (figure 8m, n).

Discussion

This novel study describes size-based morphological characteristics of the arterial vasculature in IPF, performed through systematic classification, using appropriate quantitative measurement strategies. Noticeably, IPF patients had extensive vascular remodelling changes through increased vascular wall thickening and disruptive ECM deposition. Interestingly, these arterial remodelling changes correlated inversely with lung physiological parameters such as DLCO and FVC, and IPF patients with smoking history had worse outcomes. Further, this study highlights a clear possibility that EndMT could have a critical contribution in driving these irreversible remodelling changes for the first time. Finally, the study highlights the noticeable impact of remodelled vasculature on DLCO, indicating PH complications in IPF patients.

The study noted key histopathological remodelling changes in IPF arteries, including extensive luminal occlusion, intimal proliferation, unevenly dispersed elastin fibres, collagen fragmentation and deposition across arterial layers. In addition, the adventitia was found to be incessantly merged into surrounding fibrotic areas. Such features are classic reminiscent of arteries in IPF lungs and very similar as noted in PH-COPD and PH-IPF lungs [18] pathology, suggesting a strong relationship between the two pathologies [12, 18]. Furthermore, we identified regression in numbers of medium and large muscular arteries in IPF patients, likely

resulting from intense fibrotic remodelling damage or lack of physical space for further arterial expansion. Previous similar findings of such arterial obliteration have been featured in emphysema patients with severe PH [19]. Interestingly, our observation of a much lower decline in smaller arteries illustrates heterogeneity in arterial formation. Earlier, findings on vascular formation in IPF are contradictory, with Keane et al. [20] demonstrating augmented angiogenic activity. In contrast, others have documented a decline in vessel formation, identified primarily through lower vascular endothelial growth factor levels in bronchoalveolar lavage of IPF patients [21, 22]. Also, our study found no apparent differences between total arterial thickness across the sizes in fibrotic areas and the more normal non-fibrotic areas. Although only a few areas with corresponding arterial sizes were available, our analysis suggests that such remodelling change, at least in the late stage of IPF, does not differ based on the fibrotic status and would represent the pathological changes in its entirety. Future studies with tissues from comparing early and late-stage fibrotic vs non-fibrotic areas could better predict pathological arterial remodelling.

The arterial architecture comprises three layers, the inner intima constituting endothelial cells, the medial smooth muscle layer bounded by elastin laminas, and the outer adventitial, mainly connective tissues [23]. Any configurational change to these layers affects the overall oxygenation, leading to severe hypoxic conditions. Our assessment of the arteries revealed thickening of the layer across arterial sizes in IPF lungs compared to healthy controls. Specifically, our data suggest a more considerable intimal thickening than the media and adventitia layer across the arterial sizes than seen in healthy subjects. Few previous studies have made such extensive and critical analyses of the IPF arteries. Our findings are in contrast with the previous finding by Kinoshita et al.[16], who identified significant increases in the adventitia, than in intima and media thickening in their patient cohort and, to an extent, are in concurrence to Hoffman et al. [24] finding who identified an increase in intima and media but not in the adventitia in the IPF-PF cohort of patients. However, both studies lacked essential correlation to human lung physiological parameters, which is critical in the clinical understanding of the disease progression and addressed in the current study.

The heightened activity of the endothelium in the intima and their aggressive encroachment into luminal space can be attributed to their transformative ability into a more proliferative phenotype; however molecular exploration into such endothelial cell changes in IPF is still warranted [24]. Several growth factors and signalling mechanisms, including TGFβ, hedgehog (SHH), and notch, are highly active in IPF tissues and are crucial to endothelial to mesenchymal

transition (EndMT) and proliferation [25, 26]. Similar factors could be contributing to medial and adventitial thickening, wherein smooth muscle hypertrophy and fibroblast hyperplasia were exhibited in our study of the IPF arteries [23, 27]. An interesting study by Arribas et al. [28] in a rat hypertension model showed that the adventitial thickening occurred well before changes in intima or media occurred, actively causing arterial remodelling and PH. The inter-dynamics of arterial layers and their cause-and-effect relation on overall vascular thickening remain underexplored and requires further understanding in IPF.

Elastin fibres maintain the structural integrity of the vasculature. In normal arteries, the internal and external elastin laminas consist of mature elastic fibres that offer elasticity to the vascular tissue. Their fragmentation or aberrant deposition can adversely affect elastic recoil and other vascular mechanical properties [29, 30]. Our study identified increased accumulation and elastin breakdown across arterial layers and sizes in IPF patients. Our data support the observation of Kinoshita et al. [16] of medial elastosis in IPF patients; however, unlike their findings, our study showed more significant elastin deposition in the intimal layer than in media and adventitia, especially in medium and large arteries. The increased presence of elastin, either as fragments or elastic laminal thickening, can aid endothelial migration and enhance metalloprotease activities [31, 32]. Minkin et al. demonstrated the elastin degradation products such as desmosine and isodesmosine in urine and blood samples from PAH diagnosed patients [33]. The presence of elastin fragments in the circulation activates cytokines and associated signalling pathways that can further degrade elastic fibres [31]. Both elastin and collagen contribute to the arterial thickening and PAH development in humans [34]. Poiani et al. [35] in hypoxia-induced PH rat models showed increased accumulation of elastin and collagen in pulmonary arteries. Several in-vitro studies previously have demonstrated that a poor oxygen environment is conducive to fibroblast proliferation and ECM accumulation [36, 37]

Lung physiological tests such as FVC and DLCO are used to assess IPF patient's lung function. In IPF patients, these lung function parameters are adversely affected. Reduced DLCO out of proportion to the underlying pulmonary fibrosis, a sign of concomitant PH [27]. Nadrous et al. also observed frequent PH in advanced IPF correlated with low DLCO, low resting and arterial oxygen tension (P_{aO2})[38]. Our study data confirms significant vascular remodelling changes such as increased arterial thickness and elastin negatively influenced DLCO and FVC in IPF patients. Reduction in arterial numbers and luminal size was also observed to impact DLCO adversely. Occlusive venopathy has also been observed in non-fibrotic lung areas of IPF patients, suggesting that the reduction in pulmonary capillary blood volume is due to occlusive

venopathy and related to low DLCO values in the IPF-PH patients [12]. We also identified that smoking impacted arterial thickness and elastin deposition similar to those reported in COPD patients associated with PH comorbidities [39].

Our descriptive observations indicate the increased presence of mesenchymal cells in the intima, media and adventitia layers, implying mesenchymal transformation in vascular cells [7]. The intimal mesenchymal marker expression was the highest among the three layers, indicating possible endothelial cell transition through the EndMT process [40-43]. In media and adventitia, the presence of mesenchymal cells markers such as N-cadherin, Vimentin and S100A4 was intriguing and pointed towards either resident cell transformation to mesenchymal cells or active inward migration of transitioning endothelial cells; however, these indications need further in-depth verifications. Interestingly, we also observed the increased cytoplasmic expression of VE-cadherin rather than junctional in IPF endothelial cells, indicating possible active cellular uptake of this protein. Furthermore, we demonstrate increase in α-SMA+ expression prominently in the intimal layer of IPF arteries, suggesting inadvertent myofibroblast proliferation. The myofibroblasts are highly active form of fibroblast known to aberrantly secrete ECM protein, causing thickening and stiffening of tissues [17]. The increase in collagen type-I and IV's aberrant and disruptive deposition is possibly linked to αSMA+ myofibroblasts; however, the source of these cells requires further investigation. Together with other cell types, transitioning endothelial cells could majorly contribute to the arterial remodelling and fibrotic pathology observed in IPF. Thus, we postulate the substantial involvement of EndMT in arterial remodelling and its possible role in PH and other lung complications.

The limitation of this study includes the number of IPF, and NC samples varies for size-based comparison as some arterial sizes were not found in IPF and NC tissues. Another limitation is the non-availability of cardiac function data or the clinical diagnosis of PH for the IPF patients studied, and as such, these associations could not be established in this study. However, the negative correlation of vascular remodelling with DLCO indicates possible PH in IPF patients.

In summary, this study provides important morphometric data on the remodelling of muscular arteries in the IPF lung. More importantly, we have identified that such change directly resulted in physiological change, deficient oxygen absorption, and lung capacity. EndMT seems central to IPF pathology and could be a novel therapeutic target. Thus, our data would support the need

for diagnosis and therapeutic options for vascular remodelling, which might occur with IPF prognosis and future complications.

Funding: This work was supported by research grants from Clifford Craig Foundation, Launceston General Hospital and Lung Foundation Australia.

Acknowledgments: Archana Vijay Gaikwad, Wenying Lu and Mathew Suji Eapen are thankful to the National Health and Medical Research Council (NHMRC) Centre of Research Excellence (CRE) in Pulmonary Fibrosis (Australia) for the CREATE Fellowship.

Financial/nonfinancial disclosures

Sukhwinder Singh Sohal reports personal fees for lectures from Chiesi outside the submitted work. All the other authors do not have any conflict of interest to declare.

Table 1: Subject Demographics and Clinical Characteristics

	Normal Control (NC)	**IPF**
Factor	Values *	
Total Number (n)	11	13
Age	41 ± 15.1	64 ± 5.06
Gender (F/M)	6/5	6/7
Body Mass Index	NA	26.69 ± 3.03
Smoking Status: Current, Ex-smoker and Never (n)	non-smokers	0/7/6
Smoking pack-years	-	20.84 ± 23.16
Lung physiology		
FEV_1 (L)	-	1.70 ±0.40
FEV_1 (%) Predicted	-	60.17 ±12.22
FVC (L)	-	1.97±0.51
FVC (%) Predicted	-	53.5±12.98
DLCO (ml/min/mmHg)	-	5.91±2.92
DLCO Corrected (%) Predicted	-	25.85±15.30

*Values represents the mean and the standard deviation; NA- not available

References

1. Lederer DJ, Martinez FJ. Idiopathic Pulmonary Fibrosis. *The New England journal of medicine* 2018: 378(19): 1811-1823.
2. Eapen MS, Gaikwad AV, Thompson IE, Lu W, Myers S, Sharma P, Sohal SS. The effectiveness of immunosuppressive cyclosporin in attenuating the progression of interstitial lung diseases. *Journal of Thoracic Disease* 2019: S1139-S1142.
3. Glassberg MK. Overview of idiopathic pulmonary fibrosis, evidence-based guidelines, and recent developments in the treatment landscape. *Am J Manag Care* 2019: 25(11 Suppl): S195-s203.
4. Raghu G, Remy-Jardin M, Myers JL, Richeldi L, Ryerson CJ, Lederer DJ, Behr J, Cottin V, Danoff SK, Morell F, Flaherty KR, Wells A, Martinez FJ, Azuma A, Bice TJ, Bouros D, Brown KK, Collard HR, Duggal A, Galvin L, Inoue Y, Jenkins RG, Johkoh T, Kazerooni EA, Kitaichi M, Knight SL, Mansour G, Nicholson AG, Pipavath SNJ, Buendía-Roldán I, Selman M, Travis WD, Walsh SLF, Wilson KC. Diagnosis of Idiopathic Pulmonary Fibrosis. An Official ATS/ERS/JRS/ALAT Clinical Practice Guideline. *Am J Respir Crit Care Med* 2018: 198(5): e44-e68.
5. Richeldi L, Collard HR, Jones MG. Idiopathic pulmonary fibrosis. *Lancet (London, England)* 2017: 389(10082): 1941-1952.
6. Bagnato G, Harari S. Cellular interactions in the pathogenesis of interstitial lung diseases. *European Respiratory Review* 2015: 24(135): 102-114.
7. Ghigna M-R, Dorfmüller P. Pulmonary vascular disease and pulmonary hypertension. *Diagnostic Histopathology* 2019: 25(8): 304-312.
8. Farkas L, Gauldie J, Voelkel NF, Kolb M. Pulmonary Hypertension and Idiopathic Pulmonary Fibrosis. *American Journal of Respiratory Cell and Molecular Biology* 2011: 45(1): 1-15.
9. Barratt S, Millar A. Vascular remodelling in the pathogenesis of idiopathic pulmonary fibrosis. *QJM: An International Journal of Medicine* 2014: 107(7): 515-519.
10. Nathan SD, Shlobin OA, Ahmad S, Koch J, Barnett SD, Ad N, Burton N, Leslie K. Serial development of pulmonary hypertension in patients with idiopathic pulmonary fibrosis. *Respiration* 2008: 76(3): 288-294.
11. Lettieri CJ, Nathan SD, Barnett SD, Ahmad S, Shorr AF. Prevalence and Outcomes of Pulmonary Arterial Hypertension in Advanced Idiopathic Pulmonary Fibrosis. *Chest* 2006: 129(3): 746-752.
12. Colombat M, Mal H, Groussard O, Capron F, Thabut G, Jebrak G, Brugière O, Dauriat G, Castier Y, Lesèche G, Fournier M. Pulmonary vascular lesions in end-stage idiopathic pulmonary fibrosis: histopathologic study on lung explant specimens and correlations with pulmonary hemodynamics. *Human pathology* 2007: 38(1): 60-65.
13. Sakao S, Tanabe N, Tatsumi K. Hypoxic Pulmonary Vasoconstriction and the Diffusing Capacity in Pulmonary Hypertension Secondary to Idiopathic Pulmonary Fibrosis. *Journal of the American Heart Association* 2019: 8(16): e013310.
14. Parra ER, David YR, Costa LRSd, Ab'Saber A, Sousa R, Kairalla RA, de Carvalho CRR, Filho MT, Capelozzi VL. Heterogeneous Remodeling of Lung Vessels in Idiopathic Pulmonary Fibrosis. *Lung* 2005: 183(4): 291-300.
15. Nathan SD, Noble PW, Tuder RM. Idiopathic Pulmonary Fibrosis and Pulmonary Hypertension. *Am J Respir Crit Care Med* 2007: 175(9): 875-880.
16. Kinoshita Y, Ishii H, Kushima H, Johkoh T, Yabuuchi H, Fujita M, Nabeshima K, Watanabe K. Remodeling of the pulmonary artery in idiopathic pleuroparenchymal fibroelastosis. *Scientific Reports* 2020: 10(1): 306.
17. Eapen MS, Lu W, Hackett TL, Singhera GK, Mahmood MQ, Hardikar A, Ward C, Walters EH, Sohal SS. Increased myofibroblasts in the small airways, and relationship to

remodelling and functional changes in smokers and COPD patients: potential role of epithelial–mesenchymal transition. *ERJ Open Research* 2021: 7(2): 00876-02020.
18. HEATH D, EDWARDS JE. The Pathology of Hypertensive Pulmonary Vascular Disease. *Circulation* 1958: 18(4): 533-547.
19. Adir Y, Shachner R, Amir O, Humbert M. Severe Pulmonary Hypertension Associated With Emphysema: A New Phenotype? *Chest* 2012: 142(6): 1654-1658.
20. Keane MP, Belperio JA, Burdick MD, Lynch JP, Fishbein MC, Strieter RM. ENA-78 is an important angiogenic factor in idiopathic pulmonary fibrosis. *Am J Respir Crit Care Med* 2001: 164(12): 2239-2242.
21. Meyer KC, Cardoni A, Xiang Z-Z. Vascular endothelial growth factor in bronchoalveolar lavage from normal subjects and patients with diffuse parenchymal lung disease. *Journal of Laboratory and Clinical Medicine* 2000: 135(4): 332-338.
22. Tzouvelekis A, Anevlavis S, Bouros D. Angiogenesis in Interstitial Lung Diseases: a pathogenetic hallmark or a bystander? *Respiratory Research* 2006: 7(1): 82.
23. TOMASHEFSKI JF, & DAIL, D. H. Dail and Hammar's pulmonary pathology. *Springer* 2008: Vol. 1.
24. Hoffmann J, Wilhelm J, Marsh LM, Ghanim B, Klepetko W, Kovacs G, Olschewski H, Olschewski A, Kwapiszewska G. Distinct Differences in Gene Expression Patterns in Pulmonary Arteries of Patients with Chronic Obstructive Pulmonary Disease and Idiopathic Pulmonary Fibrosis with Pulmonary Hypertension. *Am J Respir Crit Care Med* 2014: 190(1): 98-111.
25. Gaikwad AV, Eapen MS, McAlinden KD, Chia C, Larby J, Myers S, Dey S, Haug G, Markos J, Glanville AR, Sohal SS. Endothelial to mesenchymal transition (EndMT) and vascular remodeling in pulmonary hypertension and idiopathic pulmonary fibrosis. *Expert Review of Respiratory Medicine* 2020: 14(10): 1027-1043.
26. Liu G, Philp AM, Corte T, Travis MA, Schilter H, Hansbro NG, Burns CJ, Eapen MS, Sohal SS, Burgess JK, Hansbro PM. Therapeutic targets in lung tissue remodelling and fibrosis. *Pharmacology & Therapeutics* 2021: 225: 107839.
27. Ruffenach G, Hong J, Vaillancourt M, Medzikovic L, Eghbali M. Pulmonary hypertension secondary to pulmonary fibrosis: clinical data, histopathology and molecular insights. *Respiratory Research* 2020: 21(1): 303.
28. Arribas SM, Hillier C, González C, McGrory S, Dominiczak AF, McGrath JC. Cellular aspects of vascular remodeling in hypertension revealed by confocal microscopy. *Hypertension (Dallas, Tex : 1979)* 1997: 30(6): 1455-1464.
29. Karnik SK, Brooke BS, Bayes-Genis A, Sorensen L, Wythe JD, Schwartz RS, Keating MT, Li DY. A critical role for elastin signaling in vascular morphogenesis and disease. *Development (Cambridge, England)* 2003: 130(2): 411-423.
30. Roger Parra E, Adib Kairalla R, de Carvalho CRR, Capelozzi VL. Abnormal deposition of collagen/elastic vascular fibres and prognostic significance in idiopathic interstitial pneumonias. *Thorax* 2007: 62(5): 428-437.
31. Cocciolone AJ, Hawes JZ, Staiculescu MC, Johnson EO, Murshed M, Wagenseil JE. Elastin, arterial mechanics, and cardiovascular disease. *American Journal of Physiology-Heart and Circulatory Physiology* 2018: 315(2): H189-H205.
32. Skeie JM, Mullins RF. Elastin-Mediated Choroidal Endothelial Cell Migration: Possible Role in Age-Related Macular Degeneration. *Investigative Ophthalmology & Visual Science* 2008: 49(12): 5574-5580.
33. Minkin R, Grosu H, Tartell L, Ma S, Lin YY, Eden E, Turino GM. Detection of Elastin Degradation Products in the Blood and Urine of Patients With Pulmonary Arterial Hypertension. *Chest* 2010: 138(4, Supplement): 891A.

34. Rabinovitch M. PATHOBIOLOGY OF PULMONARY HYPERTENSION: Extracellular Matrix. *Clinics in Chest Medicine* 2001: 22(3): 433-449.
35. Poiani GJ, Tozzi CA, Yohn SE, Pierce RA, Belsky SA, Berg RA, Yu SY, Deak SB, Riley DJ. Collagen and elastin metabolism in hypertensive pulmonary arteries of rats. *Circulation Research* 1990: 66(4): 968-978.
36. Das M, Dempsey EC, Bouchey D, Reyland ME, Stenmark KR. Chronic hypoxia induces exaggerated growth responses in pulmonary artery adventitial fibroblasts: potential contribution of specific protein kinase c isozymes. *Am J Respir Cell Mol Biol* 2000: 22(1): 15-25.
37. Falanga V, Kirsner RS. Low oxygen stimulates proliferation of fibroblasts seeded as single cells. *Journal of cellular physiology* 1993: 154(3): 506-510.
38. Nadrous HF, Pellikka PA, Krowka MJ, Swanson KL, Chaowalit N, Decker PA, Ryu JH. The impact of pulmonary hypertension on survival in patients with idiopathic pulmonary fibrosis. *Chest* 2005: 128(6 Suppl): 616s-617s.
39. Peinado VI, Pizarro S, Barberà JA. Pulmonary Vascular Involvement in COPD. *Chest* 2008: 134(4): 808-814.
40. Sohal SS. Endothelial to mesenchymal transition (EndMT): an active process in Chronic Obstructive Pulmonary Disease (COPD)? *Respiratory Research* 2016: 17(1): 20.
41. Sohal SS. Epithelial and endothelial cell plasticity in chronic obstructive pulmonary disease (COPD). *Respiratory investigation* 2017: 55(2): 104-113.
42. Eapen MS, Myers S, Lu W, Tanghe C, Sharma P, Sohal SS. sE-cadherin and sVE-cadherin indicate active epithelial/endothelial to mesenchymal transition (EMT and EndoMT) in smokers and COPD: implications for new biomarkers and therapeutics. *Biomarkers : biochemical indicators of exposure, response, and susceptibility to chemicals* 2018: 23(7): 709-711.
43. Eapen MS, Lu W, Gaikwad AV, Bhattarai P, Chia C, Hardikar A, Haug G, Sohal SS. Endothelial to mesenchymal transition: a precursor to post-COVID-19 interstitial pulmonary fibrosis and vascular obliteration? *European Respiratory Journal* 2020: 56(4): 2003167.
44. Siow RC, Mallawaarachchi CM, Weissberg PL. Migration of adventitial myofibroblasts following vascular balloon injury: insights from in vivo gene transfer to rat carotid arteries. *Cardiovascular research* 2003: 59(1): 212-221.
45. Li G, Chen SJ, Oparil S, Chen YF, Thompson JA. Direct in vivo evidence demonstrating neointimal migration of adventitial fibroblasts after balloon injury of rat carotid arteries. *Circulation* 2000: 101(12): 1362-1365.

a)

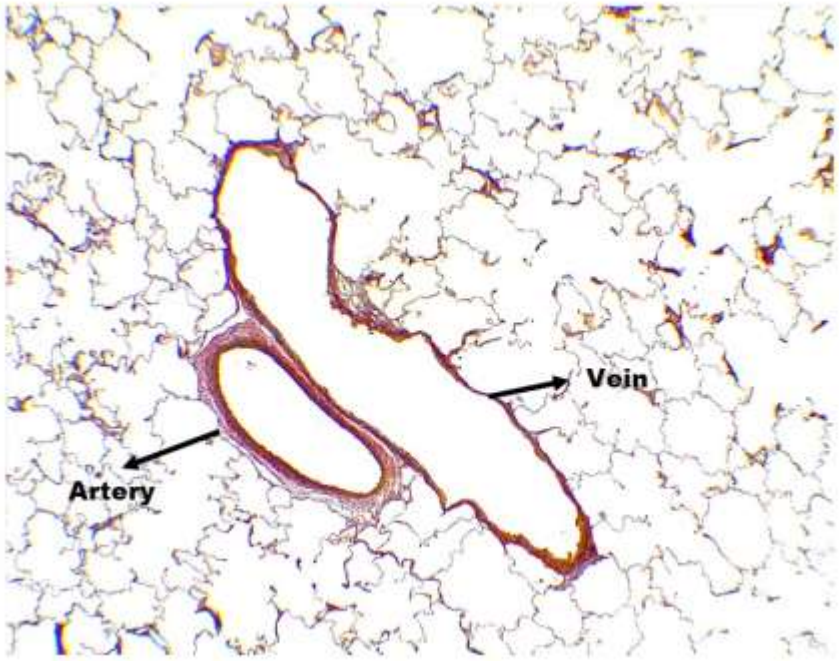
Vein
Artery

b)

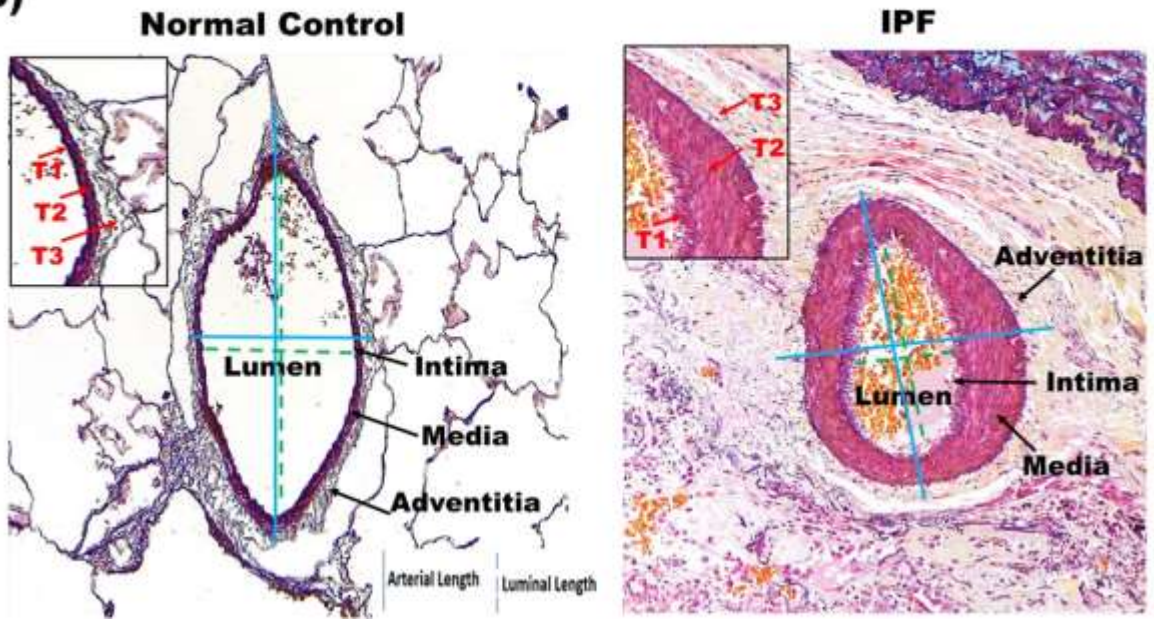
Normal Control
IPF
T1
T2
T3
Lumen
Intima
Media
Adventitia
Arterial Length
Luminal Length
T3
T2
T1
Adventitia
Lumen
Intima
Media

Figure 1a) Illustration of the normal pulmonary artery and vein structure stained with Movat Pentachrome (4x magnification). The pulmonary arteries are well rounded in structure, while veins are elongated and irregular. **b)** Movat Pentachrome stained normal control and IPF of pulmonary arteries external and luminal length measurement (20x magnification). External length is measured from one end to the other end of the adventitia layer margin crossing the middle of the lumen, while the luminal length was measured from one end to another end of the intima layer margin. In the inset are various layers (T1- Intima, T2- Media and T3- Adventitia) thickness.

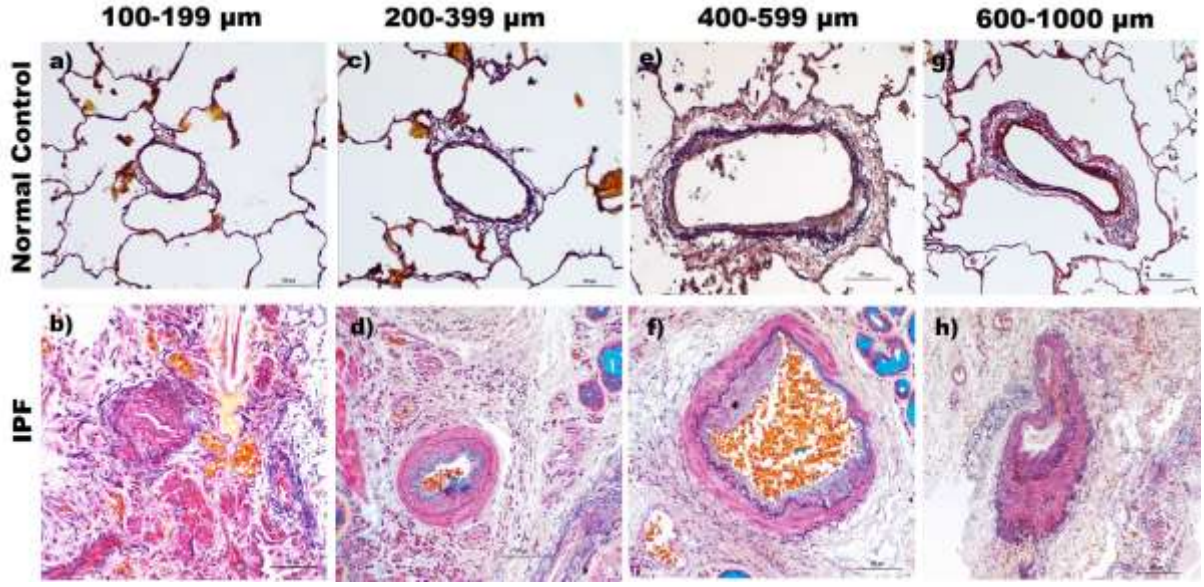

Figure 2 Representative images of Movat pentachrome stained pulmonary artery sizes for NC and IPF **(a-b)** 100-199 µm **(c-d)** 200-399 µm and **(e-f)** 400-599 µm (20x magnification) and **(g-h)** 600-1000µm (10x magnification). The prominent intimal thickening and luminal narrowing in IPF patients across various sizes are noted. Also noticed is the arterial adventitia area merging into the surrounding lung tissues in IPF patients. *Shows plexiform in figure (f).

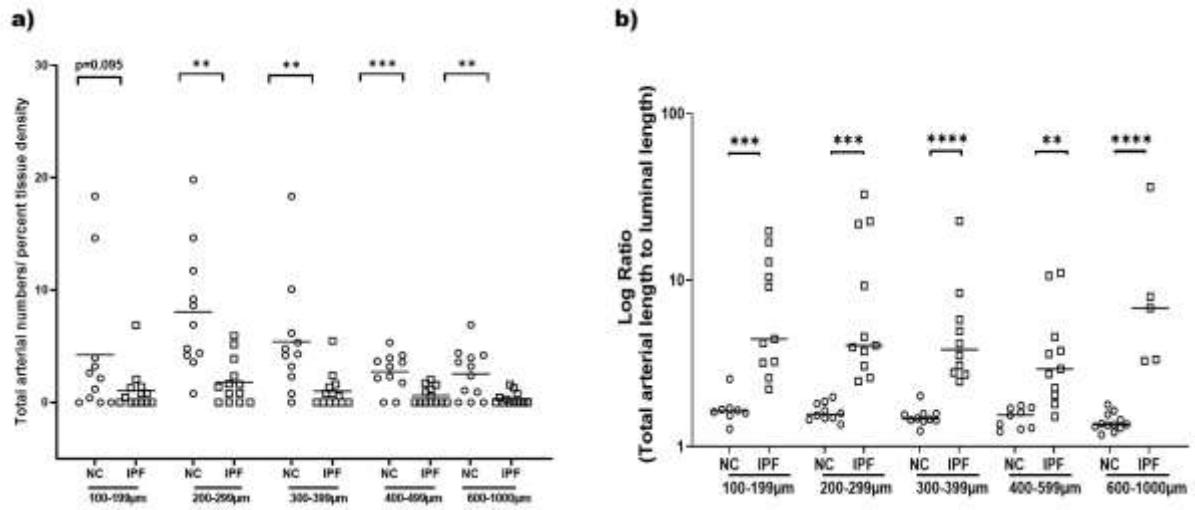

Figure 3 a) Quantitative assessment of the total number of arteries in IPF and NC across classified arterial sizes and **b)** arterial length to luminal length log ratio of pulmonary arteries across the classified arterial sizes of IPF compared to NC. Data are presented as log ratio with Unpaired T-test between each arterial classified size for NC and IPF; *p < 0.05, **p<0.01, ***p<0.001, ****p<0.0001 was considered significant.

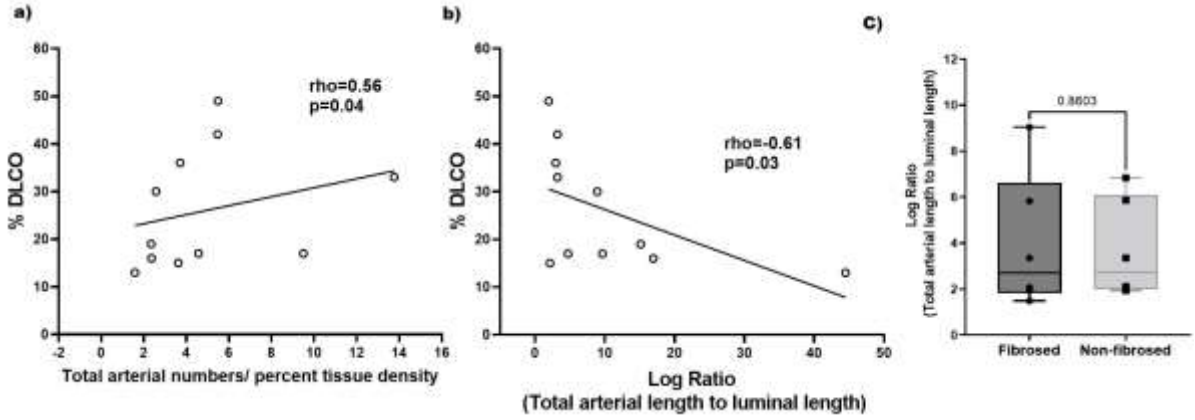

Figure 4 Correlations between **a)** total arterial numbers/ mean per cent tissue density and % DLCO **b)** total arterial length to luminal length log ratio and % DLCO and **c)** total arterial length to luminal length ratio for arteries from fibrosed and non-fibrosed area in IPF.

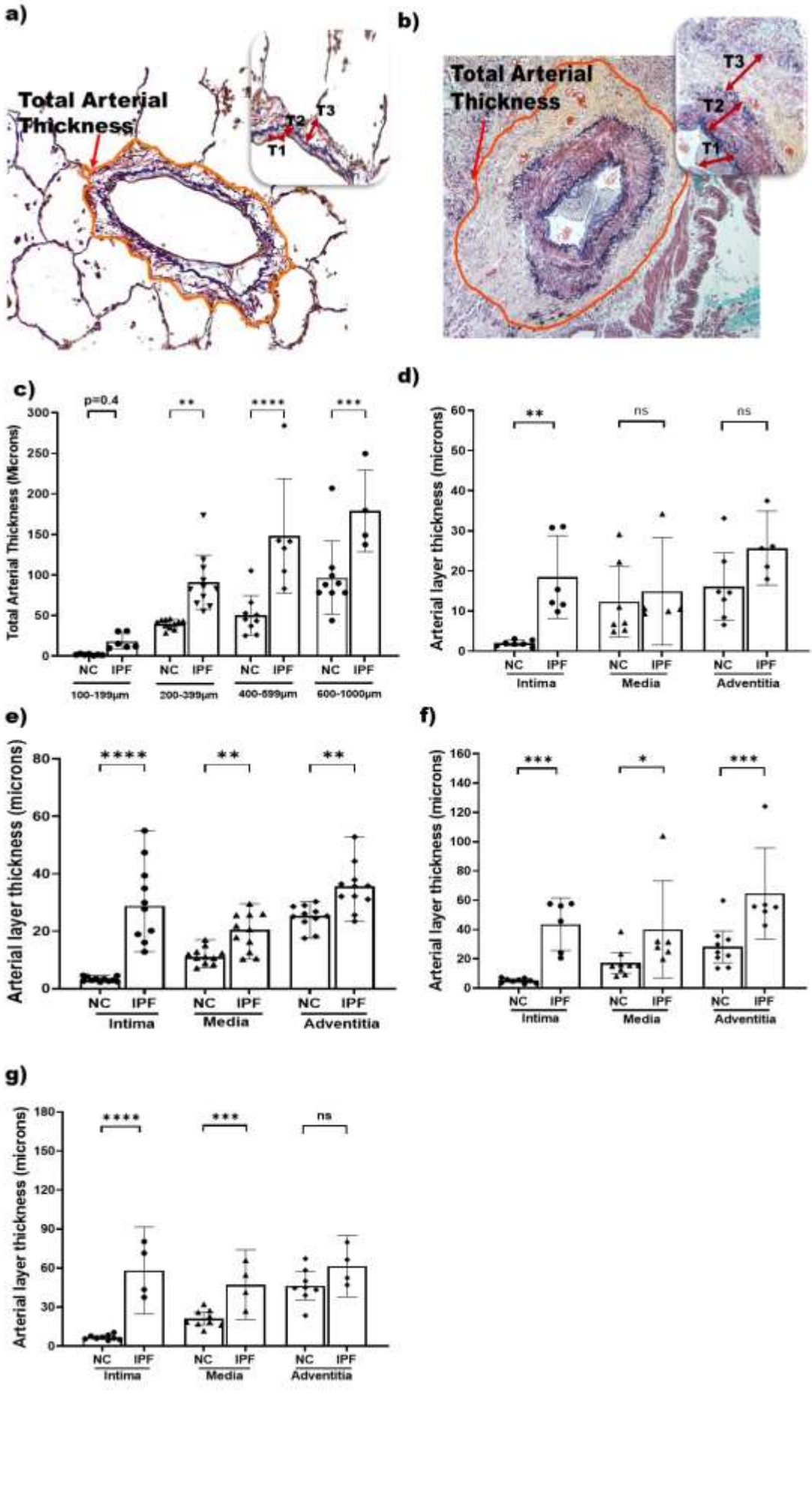
a)
Total Arterial Thickness
T1
T2
T3
b)
Total Arterial Thickness
T1
T2
T3
c)
Total Arterial Thickness (Microns)
p=0.4
**
****
***
NC
IPF
100-199µm
200-399µm
400-599µm
600-1000µm
d)
Arterial layer thickness (microns)
**
ns
ns
Intima
Media
Adventitia
e)
Arterial layer thickness (microns)
****
**
**
Intima
Media
Adventitia
f)
Arterial layer thickness (microns)
***
*
***
Intima
Media
Adventitia
g)
Arterial layer thickness (microns)
****
***
ns
Intima
Media
Adventitia

Figure 5 a, b) Arterial layer thickness measurement strategy in NC and IPF. Total arterial thickness was measured by selecting total arterial circumference. In the inset are various layers (T1- Intima, T2- Media and T3- Adventitia) thickness. Morphometric changes in arterial layers among **c**) total arterial thickness across arterial size 100-1000µm **d)** 100-199µm, **e)** 200-399µm, **f)** 400-599µm and **g)** 600-1000µm. All data are presented as multiple comparisons with Ordinary one-way ANOVA; $p < 0.05$ was considered significant.

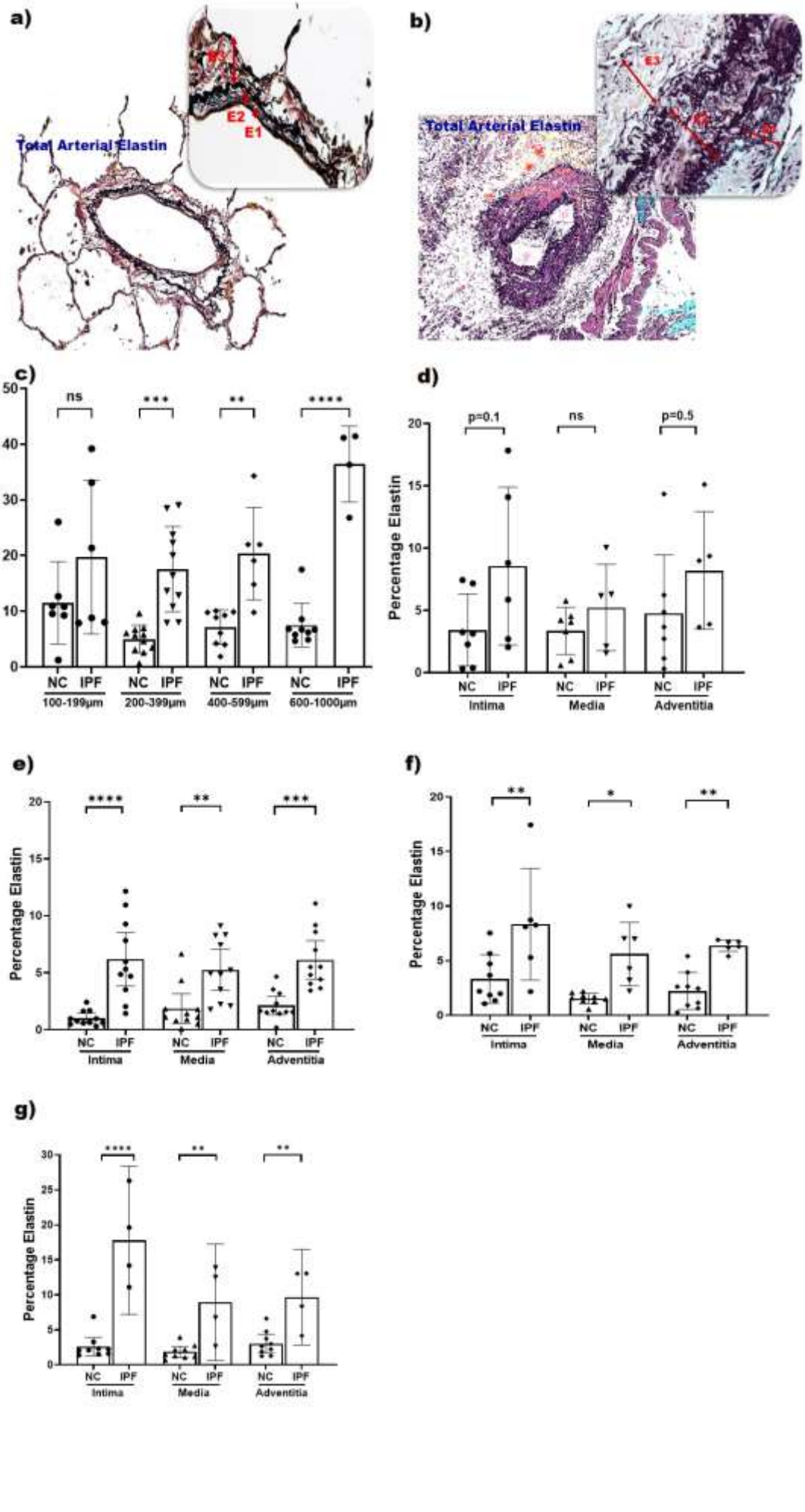
a)
Total Arterial Elastin
E3
E2
E1
b)
Total Arterial Elastin
E3
E2
E1
c)
Total Elastin Percentage
ns
***
**
****
NC IPF
100-199µm
200-399µm
400-599µm
600-1000µm
d)
Percentage Elastin
p=0.1
ns
p=0.5
NC IPF
Intima
Media
Adventitia
e)
Percentage Elastin
****
**
***
NC IPF
Intima
Media
Adventitia
f)
Percentage Elastin
**
*
**
NC IPF
Intima
Media
Adventitia
g)
Percentage Elastin
****
**
**
NC IPF
Intima
Media
Adventitia

Figure 6 a, b) Arterial layer elastin measurement strategy in NC and IPF. The black colour presents the elastin count. In the inset are various layers (E1- Intima, E2- Media and E3- Adventitia) elastin. Morphometric changes in arterial layer elastin among **c)** total arterial elastin across arterial size 100-1000µm **d)** 100-199µm, **e)** 200-399µm, **f)** 400-599µm, and **g)** 600-1000µm. Arterial elastin is expressed in percentage. All data are presented as multiple comparisons with Ordinary one-way ANOVA; $p < 0.05$ was considered significant.

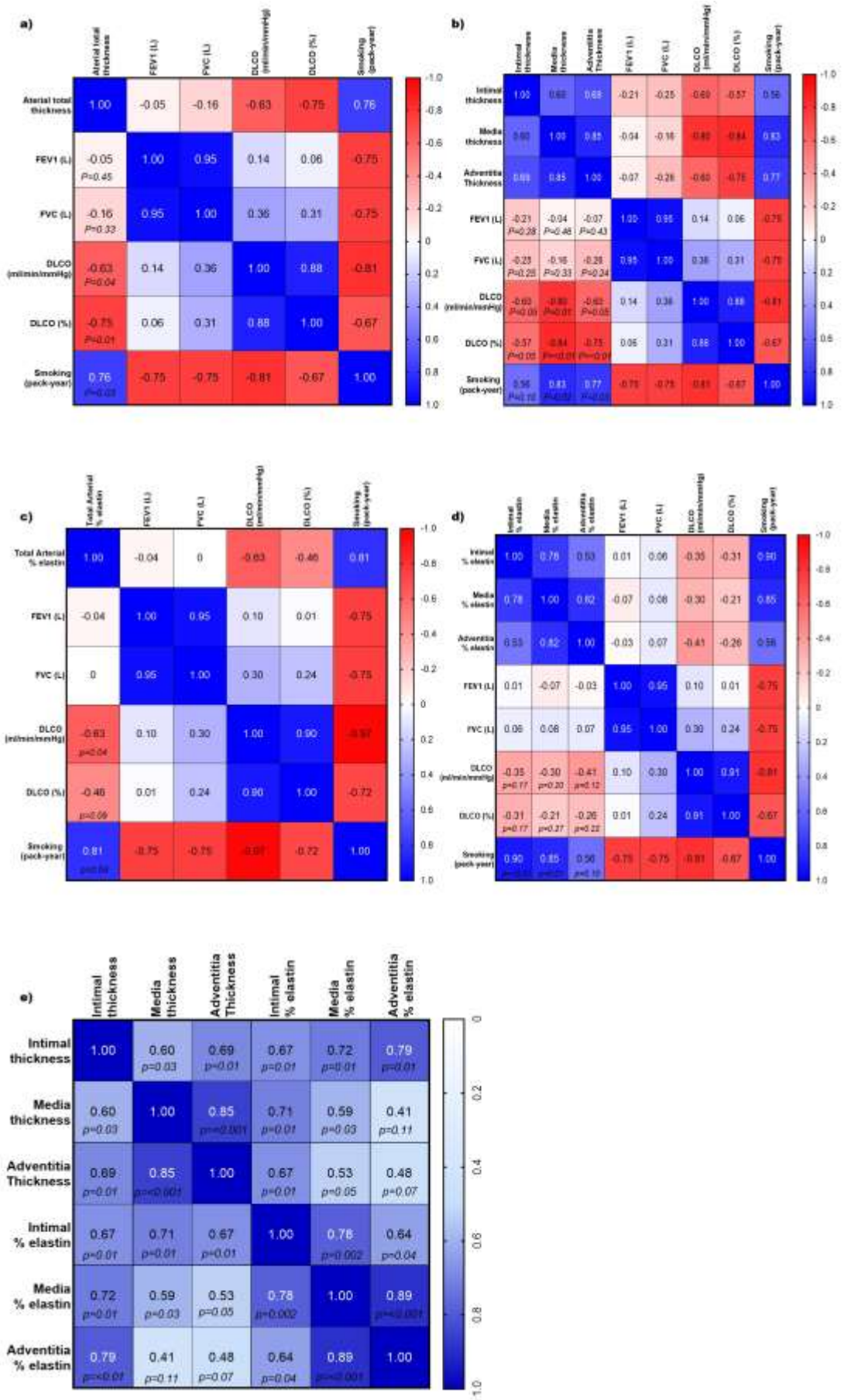

FVE1- forced expiratory volume, FVC- forced vital capacity, DLCO- diffusing capacity for carbon monoxide, PFT- pulmonary function test

Figure 7 Correlations matrix showing the impact on various measured indices on pulmonary function and smoking pack-years. **a)** pulmonary arterial total thickness, **b)** arterial individual layer thickness, **c)** pulmonary arterial total elastin, and **d)** individual arterial layer elastin **(e)** correlation between arterial thickness and arterial elastin across each arterial layer. Increased percent elastin in each layer significantly correlated to their corresponding layer thickness.

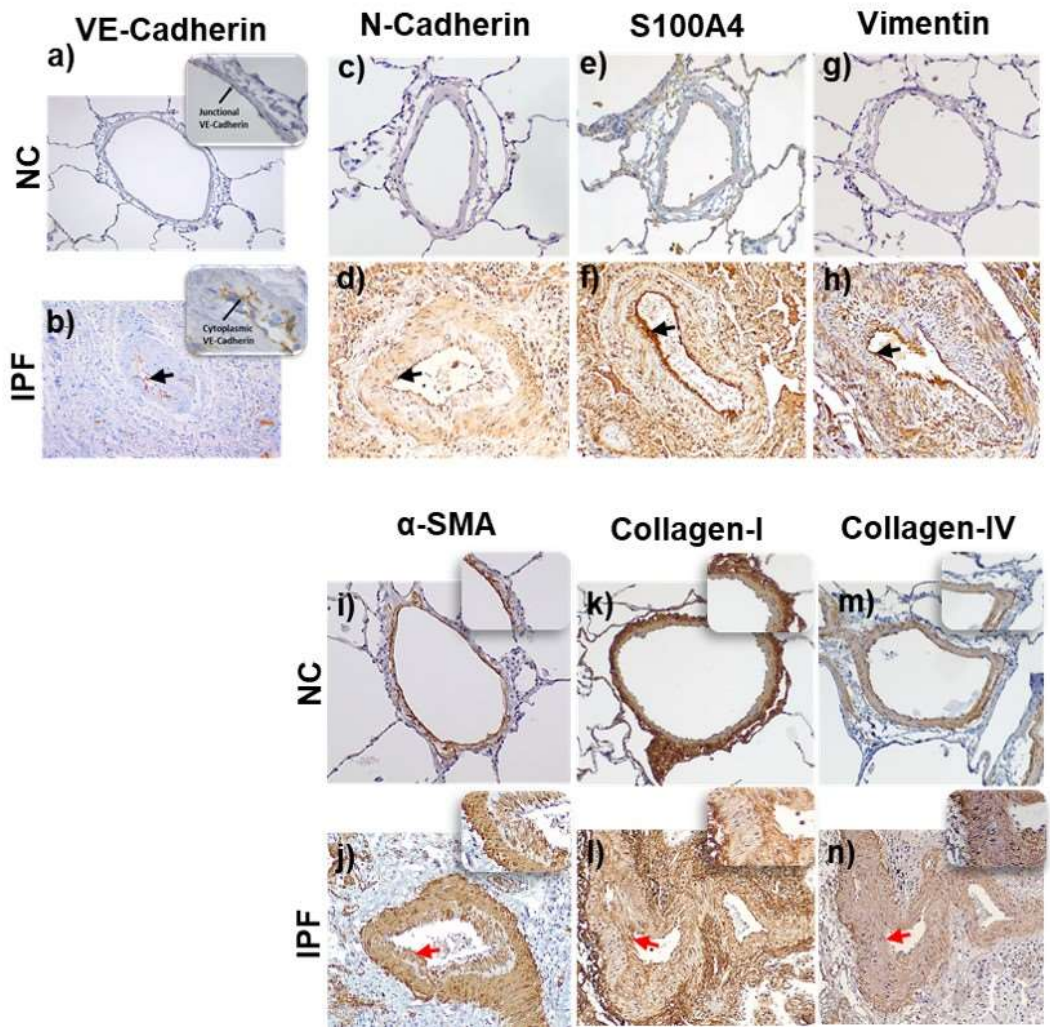

Figure 8 Descriptive images of immunohistochemically stained pulmonary arteries for VE-cadherin (Magnification 20x) **a)** NC **b)** IPF, in inset junctional and cytoplasmic expression of VE-cadherin in NC and IPF respectively (100x). Staining images for N-cadherin **c)** NC and **d)** IPF (20x), S100A4 **e)** NC and **f)** IPF, vimentin **g)** NC and **h)** IPF, for α-SMA **i)** NC and **j)** IPF collagen-I, **k)** NC and **l)** IPF and collagen-IV **m)** NC and **n)** IPF (all images taken in 20x magnification for medium size arteries). The black arrow indicates mesenchymal proteins expression in the intima, and the red arrow indicates α-SMA + myofibroblast (in inset intima) and ECM protein: collagen-I and collagen- IV deposition (in inset intima).